

# Density and compressive strength properties of polyester composites reinforced with spiral geometry woven fiber

Ergun Ateş<sup>1</sup> and Kadir Aztekin<sup>2</sup>

## Abstract

Composites can be produced by combining different materials according to different targets. In this study, woven-type E-glass fiber with a 500 g/m<sup>2</sup> unit-area weight has been used as a reinforcement material. Resin, hardener and accelerator have been used as the matrix materials. The dimensions of compression test sample molds were Ø50 mm × 100 mm. Starting from the center toward the outer diameter, spirally wound fibers have been placed into molds with intervals ranging from 1 mm to 9 mm. Composite materials have been prepared at room temperature by applying vibration to the casting method. Compression tests have been carried out on a total of 27 samples, as 3 samples per dimension. It has been determined that the compressive strengths of the polyester resin composites reinforced with spirally wound fiberglass changes per the spiral geometry. The highest compressive strength and density value have been obtained from the samples prepared with intervals of 1 mm. Compressive strength and density value curves have exhibited similar tendencies.

## Keywords

Glass fiber, polyester composite, compression, density

## Introduction

There are many different kinds of fiber-reinforced composite materials and many production methods have been developed for the production of composites with these

<sup>1</sup> Department of Mechanical Engineering, Balıkesir University, Balıkesir, Turkey

<sup>2</sup> Institute of Science and Technology, Division of Mechanical Engineering, Balıkesir University, Balıkesir, Turkey

## Corresponding author:

Ergun Ateş, Department of Mechanical Engineering, Balıkesir University, Balıkesir 10145, Turkey.

Email: eates@balikesir.edu.tr

materials.<sup>1</sup> The strengths of the composites obtained with fiber materials have to meet the levels required according to their place of use.

The reason a spiral shape was selected for this study is to examine whether the composite materials are moldable within the cylindrical external surface turning process, one of the metal-cutting methods. The composite piece is cylindrical. In every stage of the metal-removal process via tool, the depth of cut layer should be homogenous. This can only be possible if additional fibers in the composite material are produced when they are located within the spiral geometry. The scope of this study concerns the optimization of the productivity of a composite structure that encourages the best spirally geometric compression resistance necessary for the turning process. The scope is not related to the turning process or its results. No publications are available in related literature concerning the aforementioned structure formation.

The expectation of achieving the best mechanical properties also increases the amount of research conducted on this matter. Since the target in this study is the best compressive strength of fiber-reinforced materials, particularly the studies related to the basic mechanical properties have been examined.

The matrix structure in polymer concretes, fine and coarse aggregate types, binders and the distribution in the mold cavity, the formation of a loose or tight structure and the optimization of mixture rates have been studied.<sup>2-4</sup> It is a study pertaining to the determination of the damage originating from the bending fibers in kevlar-reinforced structures and the status at different temperatures. The performance of tube-shaped samples has been examined with a semistatic impact test at 25°, 55° and 75° impact angles. The effects of temperature have been less significant for the tubes at 25° and 75°. The tubes have produced the ultimate strength at a 55° angle test. Under all testing conditions, the tubes with 75° angles have been problematic and manifested fiber breakages. At 55°, the breakage mode falls dramatically from 70°C to -46°C. On the 25° tube, a substantial linear cracking has also occurred.<sup>5</sup> It is an empirical and analytic study on the bending strength of the hybrid fiber-reinforced polymer concrete (FRP) beams and bridge deck components. Although the material is coated on both the sides of a FRP layer filled with carbon-epoxy cylindrical parts, it has been structured with reinforcement. The system has been empirically examined by conducting bending tests at four points and approximate formulation, and bending results have been provided in detail with the analysis. It has been stated that the points largely affected by stress are the points drilled for connections.<sup>6</sup> The processability of the fiberglass-reinforced thermoset and thermoplastic composite materials has been studied. Drilling experiments were used a Deckel- CNC milling machine, a carbide tipped drill cutting tool (diameter 6mm, point angle 118) and cutting speed 2500rpm and feed 0.1 mm/rev. The thrust and torque are of higher order in thermoset composites. There is a significant rise in thrust and torque at around 30 holes in GF/polyester composites. This may be attributed to tool wear. This can be critical thrust for drilling of thermoset composites beyond which tool wear/delamination become dominant. Processability of the glass fiber-reinforced epoxy matrix composite pipes has been examined. Materials prepared with 30° and 90° directional fiber winding method have been processed on a conventional lathe with the use of a cermet-coated set. The test results determined that the most important parameter affecting the skin quality is the

advancement distance and that the best surface quality is obtained from 30° composite with 175 m/min shear rate, 1.5 mm cutting depth and a 0.1 mm advancement value. It has been stated that with slow shear rates, the fibers break into pieces, and due to the fact that the wide angle fibers cause compressive stress within the part, low surface quality is obtained.<sup>8</sup>

Glass-reinforced composite samples have been prepared for high compressive strengths. The structure is composed of the matrix made of two different epoxy resins along with several ossification agents and S-glass fiber as the reinforcement element. Properties such as tensile strength, flexibility, impact, hardness and glass transition temperature have been studied. Superior mechanical properties have been exhibited with high material density and low free volume. It has been determined that ossification agents are effective on the compressive strengths of the composites.<sup>9</sup> Fiber composites exhibit similar properties on many terms with materials such as wood or bone. Composites are materials that can be produced in a lightweight, robust and durable form. The solids in nature have a strong and good structure. By formulating new compositions, composites that have some additional properties similar to those in natural materials, such as less brittleness, can be produced. In general, composite structures are anisotropic and heterogeneous.<sup>10</sup> A micromechanical model that is capable of estimating the compressive strengths of the layered composites with one-way fibers has been prepared. Within the layered composite fibers are positioned the small vertical angles varying from 1° to 5°. Fiber is under shearing and buckling stresses. By considering that fibers and matrix are originated as a result of a shearing deformation, shearing buckling load has been determined by means of an energy approach.<sup>11</sup> The load–unload effect implemented with the fiber-reinforced polymer composite plates with varying values between 0.8 GPa and 1.8 GPa has been examined. Composite material has been produced using a polymer matrix and weaving type S2 glass fiber. The findings have indicated that when the impact pressure increases from 0.8 GPa to 1.8 GPa, critical shearing resistance increases from 0.108 GPa to 0.682 GPa.<sup>12</sup> The behavior of randomly positioned Lantana-camara fiber–reinforced composites under abrasive effects with  $200 \pm 50 \mu\text{m}$  particle dimension has been examined. The composites have been abraded with different angles (15°–90°) and velocities (48 m/s–109 m/s). The abrasion rates of the composites have increased in line with the increases in impact velocity and fiber amount. The scanning electron microscopy (SEM) images of the abraded surfaces have been examined. It is believed that microcracks occur on the abrasion mechanism because of reasons such as crack formations in the fibers, disposition of the fibers, shape of the chip, and embedding of sand particles in the structure.<sup>13</sup>

Depending on the implementation conditions of the studies mentioned above, composite materials of different structures have been prepared. We have attempted to determine the load properties acting on these materials, such as the mechanical, physical, chemical and atmospheric conditions. The behavior of a material can vary according to the areas of implementation. The properties of polymer concrete, the type of all components in its structure, its form and amount can change significantly when different

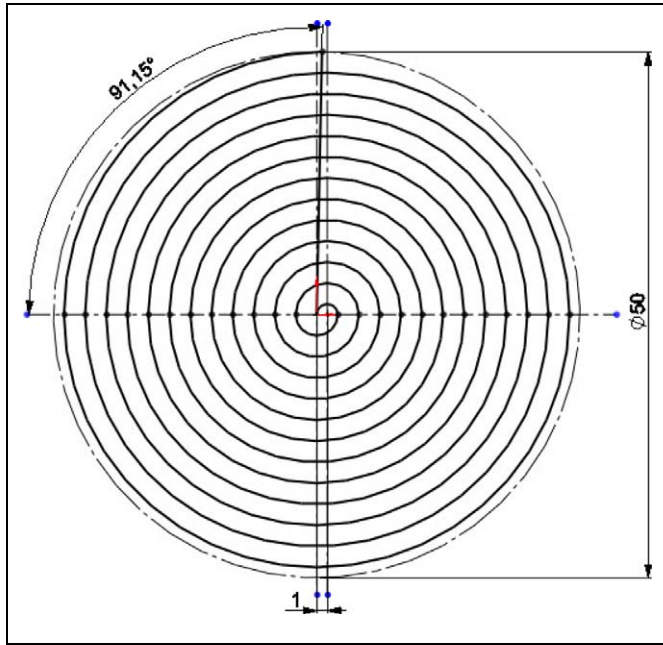


**Figure 1.** Spiral positioning with 1 mm distance between starting point and center.

production methods are adopted. Therefore, it is important to prepare the material to be produced with the most convenient solution by means of considering the differences that may be experienced in practice.

## Materials and methods

In the study, unsaturated polyester resin, hardener (methyl ethyl ketone peroxide) and accelerator (cobalt oktoat—CoOc) have been used for the matrix structure. The accelerator and hardener added to the polyester resin are catalysts. In light of the preliminary studies carried out in order to determine the rates of these materials within the composition of the structure, the rates have been determined as 98.5% polyester resin, 1% hardener and 0.5% accelerator.<sup>14</sup> Polyester resin is in compliance with the Deutsches Institut für Normung (DIN) 16911<sup>15</sup> and DIN 16945<sup>16</sup> standards.

E-glass fiber (woven roving) with a 500 g/m<sup>2</sup> unit area weight has been used as reinforcement material. The amount pertaining to this material depends on the various positions related to the formation of the spiral. The positioning details of the spirals within the molds with 1 mm intervals from 1 mm to 9 mm have been sensitively calculated with CAD software (Solid- Works, Balıkesir University, Turkey). Figure 1 shows the spiral positioning in a 50-mm diameter mold, with 1 mm distance between the starting point and the center. The horizontal axis shows the start and end of each spiral, or in other words a winding of 360°, which has been defined as a single spiral number. The

**Table 1.** Measurements of spiral positions with 1 mm increments from 1 to 9 mm.

Interval distance (mm)	Full spiral number	Increasing spiral number	Real spiral number	Increasing angle (°)	Total angle (°)	Total length (mm)
1	12	0.253	12.253	91.15	4411.15	981.25
2	6	0.172	6.172	61.97	2221.97	516.44
3	4	0.141	4.141	50.7	1490.7	360.86
4	3	0.123	3.123	44.36	1124.36	282.77
5	2	0.266	2.266	95.74	815.74	193.85
6	2	0.103	2.103	37.19	757.19	204.33
7	1	0.366	1.366	131.74	491.74	108.98
8	1	0.296	1.296	106.41	466.41	112.16
9	1	0.242	1.242	87.07	447.07	116.69

91.15° angle shown in Figure 1 is related with the final spiral in the mold that has not been fully wound and indicates the angularly measured distance in order to calculate length. This value in spiral positioning will naturally change for different starting angles. All measurement details of the spiral positions that can be done in 1 mm increments from 1 mm to 9 mm are presented in Table 1. The total length necessary to form the spiral are presented in Table 1, and their calculated values have been used in the study. Another dimension, in addition to the total length values, is the height of the woven-type E-glass fiber. This value is the height of the mold, and a fixed value of 100 mm has been used for all interval distances. The third dimension of woven-type E-glass fiber is the thickness. Regarding thickness values, the formation of a very tight structure for the compressive strength test samples to be obtained with casting has been avoided. Although woven-type E-glass fiber combines well with resin, a positioning that will allow a certain amount of polyester resin to seep in between the two spiral fiber layers has been considered. For this purpose, increments of 1 mm starting from at least 1 mm have been implemented. The thickness of the woven-type E-glass fiber used in the study is smaller than 1 mm.

The diameters of the compressive test samples are 50 mm, while their lengths are 100 mm. The dimensions selected for the compressive test are in compliance with DIN 51290-3<sup>17</sup> and ISO 4012<sup>18</sup> standards. The mold material is plastic questamide. The molds have been arranged in compliance with sample standards and sensitively processed on the lathe to achieve a 65 mm external diameter, a 50 mm internal cavity diameter, 100 mm height and 7.5 mm wall thickness. Before being cast, the molds have been subjected to a mold-release agent so that the compressive test sample set within the mold can be removed from the mold more easily. For this purpose, a thin film layer wax is applied to the molds and after 30 min of polishing, the molds become ready for casting.

Polymerization particularly starts after adding hardener into the “polyester resin + accelerator + hardener” mixture used in composing the matrix structure. The gelation time recommended by the polyester resin manufacturing company for this mixture is  $8 \pm 2$  min. The reinforcement material used in this study is woven-type E-glass fiber. The mixture has been cast on the reinforcement material previously

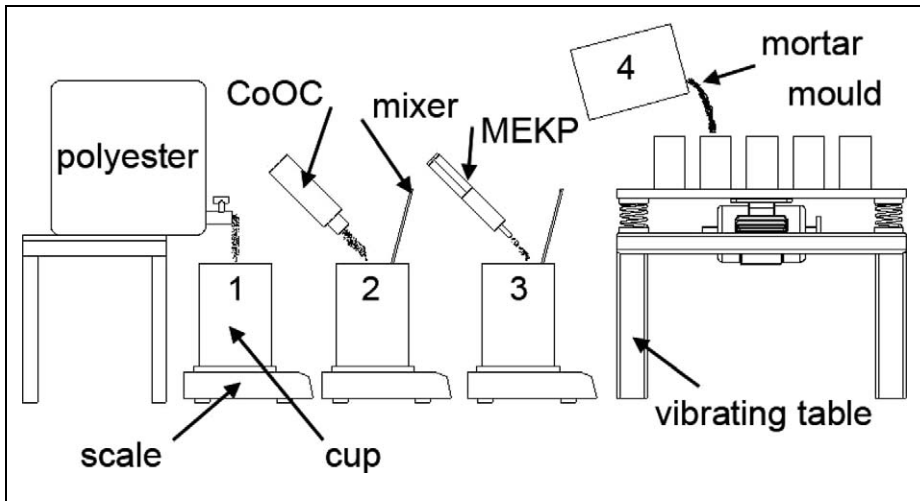


**Figure 2.** Casting steps of the spiral fiber test samples.

positioned in a spiral form within the mold. It is critical not to have any air bubbles within the structure. For this purpose, 8 min of a vibration application that allows air to release has been applied. A table-type vibrator with dimensions of 580 mm × 340 mm has been utilized for vibration. The table is connected to the bench bed with four springs. The propulsion of the table is generated by a motor with 1.5 kW power and 3000 r/min. All processing stages are schematically illustrated with four steps in Figure 2.

After casting, the compressive test samples are kept at room temperature for a total of 7 days, and 1 of the test samples are kept in the molds. On the 8th day, it is removed from the molds. A scale with 0.05 g sensitivity was used for all weighing processes and determining the density. Before the compressive test, the weights of all samples are recorded. The structure of test specimens were E-glass fibre reinforced polyester resin matrix. It is known that dimensions of the polyester resin matrix composites with or without reinforcement slightly shrink. Therefore, this slight change in dimensions affect the accounts of the density and compressive strength measurements were made at some of the dimensions of the samples are ready for the discharge experiment. A caliper gauge with 0.02 mm sensitivity has been used for dimension measurements. For the diameter of the sample, the average of the three measurements from both ends and the middle was taken. For height, the arithmetic average of three measurements each at 120° from the sample diameter was taken. Figure 3 illustrates some samples ready for the compressive tests.

Compressive tests of the samples, the dimensions of which had been completed, have been carried out with a testing machine of 3000 kN capacity. The load applied to all samples was with fixed at 50 daN/s loading velocity. With 3 samples for each spiral interval, a total of 27 samples have been studied for 9 separate interval values. Figure 4 illustrates a deformed sample after the compressive test.



**Figure 3.** Spiral-fiber–reinforced compressive test samples.



**Figure 4.** Sample after compressive test.

### **Results and discussion**

The examination of the composite structure is carried out in two stages. In the first part, the data are evaluated, graphics are drawn according to the related parameters and these

graphics are then analyzed. In the second part, the images of the composite structure that have been acquired by a SEM are examined and analyzed.

### *Evaluation of the data*

Spiral-fiber-reinforced compressive test samples have a transparent and glassy structure that turns purple due to the polyester, catalysts and particularly the CoOc used. Fibers can be easily observed in the structure. Although the samples that were deformed after the compressive test manifest a glassy brittleness, due to the fibers in it, it can retain its form without falling into pieces. During the deformation process in the compressive test, the peak resistance value is exceeded for most of the samples with a burst. At this moment, the particles may be projected. This generally applies to the fibers in the outer wall of the sample. Carrying out the compressive tests on a platform with protected perimeters is important in order to avoid accidents. Although conventional breakages are observed in the samples, it is also observed that at least three significant cracks are formed along its height. The spiral fiber reinforcement can be acknowledged as the reason for this.

The density and compressive strength values of the woven fiber-reinforced spiral composite samples obtained after the tests are given in Table 2. At this point, the study continued the evaluation from two perspectives. While one was the determination of density and the other was compressive strength value. For each spiral interval, the arithmetic averages of three samples have been used. Using this method, nine density and nine compressive strength values were obtained.

The weights of the samples were expressed in grams using a precision balance. The volumes of the test samples have been expressed as  $\text{cm}^3$ , using the sensitively measured lengths and diameters of the samples. The densities of the samples are derived by dividing the weights of the samples by their calculated volumes and are expressed in  $\text{g}/\text{cm}^3$ .

Figure 5 presents the changes in density values based on spiral intervals. Examining the changes in the test samples according to spiral interval values shows that the densities decreased in the samples with spiral intervals from 1 mm to 4 mm. Although the samples with 5 mm, 7 mm and 9 mm spiral intervals have high-density values, the samples with 6 mm and 8 mm spiral intervals demonstrated low-density values. Samples with a 1-mm spiral interval have proven to be the samples with the highest density ( $1.268 \text{ g}/\text{cm}^3$ ). While on the other hand, the samples with an 8-mm spiral interval have proved to be the samples with lowest density ( $1.190 \text{ g}/\text{cm}^3$ ). It was observed that in the graphic where the spiral interval is between 2 and 9 mm, the density changes with an average value interval of  $1.20 \text{ g}/\text{cm}^3 (\pm 0.01)$  as a band. When the spiral interval 1-mm specimens, were obtained, the largest intensity value. The density of the woven-type E-glass fiber used in the study is  $2.54 \text{ g}/\text{cm}^3$ .<sup>19</sup> On the other hand, the density of the formed plain polymer matrix is  $1.211 \text{ g}/\text{cm}^3$ .<sup>14</sup> The samples with 1-mm spiral interval constitute the group with the longest and heaviest woven-type E-glass fiber. Accordingly, this is the reason for the increase in density. While the 3- to 9-mm spiral interval values are close to each other in terms of length, it increases even further in the order of 2 mm and 1 mm (Table 1).



**Table 2.** Density and compressive strength of the woven-type fiber-reinforced spiral samples.

Spiral interval (mm)	Density (g/cm <sup>3</sup> )	Average density (g/cm <sup>3</sup> )	Compressive load (daN)	Compressive strength (N/mm <sup>2</sup> )	Compressive strength average (N/mm <sup>2</sup> )
1	1.277	1.268	15,660	79.775	82.953
	1.259		16,420	82.698	
	1.267		17,210	86.387	
2	1.204	1.206	8990	45.006	47.175
	1.217		9170	46.557	
	1.198		10,000	49.962	
3	1.200	1.195	6640	33.397	40.195
	1.184		7410	37.571	
	1.201		9720	49.616	
4	1.205	1.194	4760	24.495	28.048
	1.198		5290	26.912	
	1.180		6500	32.737	
5	1.221	1.202	3450	18.194	23.113
	1.192		4150	21.298	
	1.194		5800	29.847	
6	1.184	1.195	2850	14.538	19.603
	1.187		4160	21.206	
	1.213		4470	23.065	
7	1.201	1.205	3480	18.215	25.051
	1.207		3780	19.962	
	1.206		7040	36.975	
8	1.182	1.190	2440	12.650	24.546
	1.205		4130	21.900	
	1.182		7560	39.089	
9	1.200	1.198	4880	25.491	29.691
	1.199		5620	29.276	
	1.196		6590	34.306	

Figure 6 presents the changes in compressive strength based on the spiral intervals. Examining the changes in the compressive test samples according to spiral interval values shows that the compressive strengths tend to decrease in groups with 1–6 mm spiral intervals. At 6 mm, contrary to the 1–6 mm intervals, the compressive strength tends to increase slightly until 9 mm. The highest compressive strength has been obtained at a 1-mm spiral interval with a value of 82.953 N/mm<sup>2</sup>. The lowest compressive strength of 19.603 N/mm<sup>2</sup> was obtained from the samples with a 6-mm spiral interval. No significant differences, in terms of increases or decreases, have been observed on the curve. The sample with 1 mm spiral intervals manifested the highest compressive strength along with the highest density value. Figure 5, the spiral in the interval from 2 to 9 mm compressive strength values corresponding to density, values as given in Figure 6, close to the values received 40.175 N/mm<sup>2</sup> and 19.603 N/mm<sup>2</sup>.

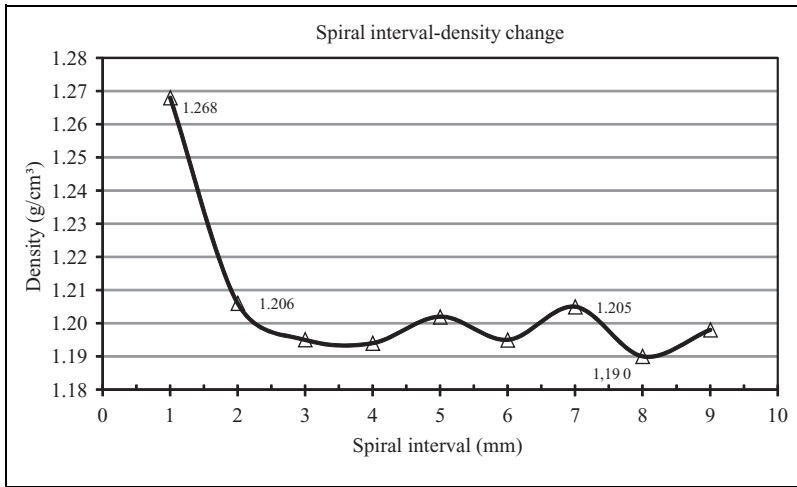


**Figure 5.** Density changes of the spirally formed composite samples depending on spiral interval.

### *SEM images and the results of the examination*

As seen in the design image (Figure 7) drawn on CAD software, the surface examinations of the composite with a SEM are initially carried out on the vertical “A” surface acquired by cutting the cylinder vertically in the direction of its axis, then on the horizontal “B” surface acquired by cutting the cylinder horizontally in the direction of its axis. As can be seen in Figure 7, the beginning of the spiral turn through the axis is always the cylinder’s axis itself. This can be seen from the central bottom point of the vertical “A” surface as shown in Figure 7. The textile-type glass fiber enlarges in spiral ranges toward the expanding diameter.

Samples were some process before the SEM imaging. the surface of the sample in this operations, cutting, coarse, medium and fine grinding and cleaning. Ethyl alcohol is used to clean the surface of the samples. The composite structure can be easily cut without great strength, and dust particles are formed after the grinding and polishing processes. The fiber and polyester chips together look like a wool spiral.

First, the “A” vertical surface is examined. The image is acquired at a magnification of  $\times 60$ . The goal was the visibility of the vertical fibers. In Figure 8, the 2 lines in the vertical direction, numbered 1 and 2 and marked by arrows, can be seen. These two lines are the image of the glass fiber on the “A” cut viewing surface. For this reason, the image is identified with the “A” sign. This image can be explicitly viewed as continuous and different particles in the structure. The direction of the glass fibers is also given as a direction under the “A” sign. The glass fibers can be clearly seen on the upper part of the image, where a bright section forms with the white-colored part. The reason behind the formation of the bright section is the fiber dust accumulation despite the polishing and cleaning processes carried out after the cutting process. The black parts seen below the image are the spaces (that are under the surface level) formed during the cutting process

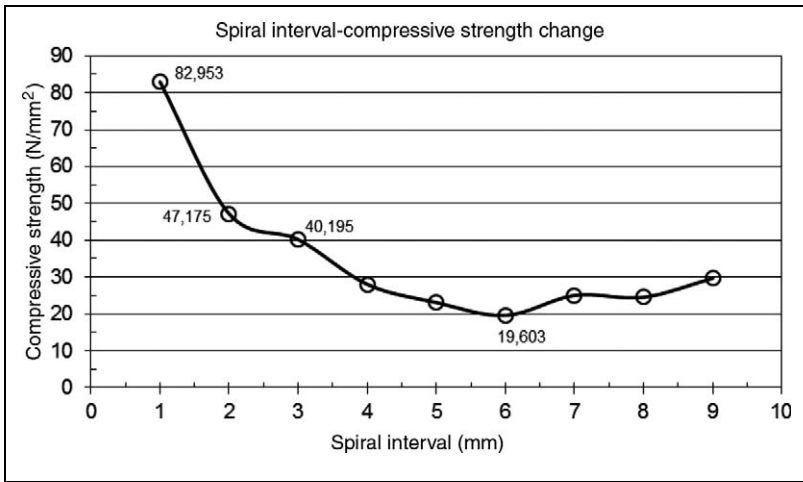


**Figure 6.** Compressive strength changes of the spirally formed composite samples depending on spiral interval.

of the structure when the surface was being prepared for imaging. The textile-type glass fibers are covered fairly well with the matrix material.

In Figure 8, a more detailed SEM image numbered 1 acquired from the horizontal line in between the two arrows can be seen. Figure 9 with “A1” sign is with a magnification of  $\times 340$ . Figure 9 provides a more detailed examination of the glass fibers in the structure. Textile glass fibers are again vertical. The spiral-shaped, less bright parts observed, particularly on the left side of the image, are the fiber and polyester dusts formed on the surface. The cut parts of the fiber viewed on the image and the black parts are the holes that are formed under the surface are due to the damage that occurred when the surface was being prepared for SEM. In fact, it could have been possible to coil the glass fibers free of damage and with the matrix material. This could be observed by a detailed examination of the fiber circle and the color change due to the matrix material covering any fiber after the production process, where a glass fiber can be fairly well covered.

SEM image in Figure 10, taken 30 magnification. This was shown by “B” in Figure 7, the horizontal surface. Here, the textile fibers start from the center and the fiber intervals are situated in such a way that they expand by growing until they reach the external diameter. In this stage, by coiling with the matrix material, the composite structure is formed. The reason for choosing the zooming ratio shown in Figure 10 is for the visibility of circular textile glass fibers, which is otherwise quite rough. In this image, a cut view of this circle can be easily seen. In Figure 10,  $\phi 1$ ,  $\phi 2$  and  $\phi 3$  represents the measurement of the cylinder from the central point to its current position. It can be seen that the textile glass fibers are almost perfectly covered with the matrix material. The textile glass fibers can be viewed on the surface as the lighter colored structure different from the gray-colored matrix structure. It has been possible to confirm that the thickness of the fiber taken from the image and the thickness of the real fiber are the

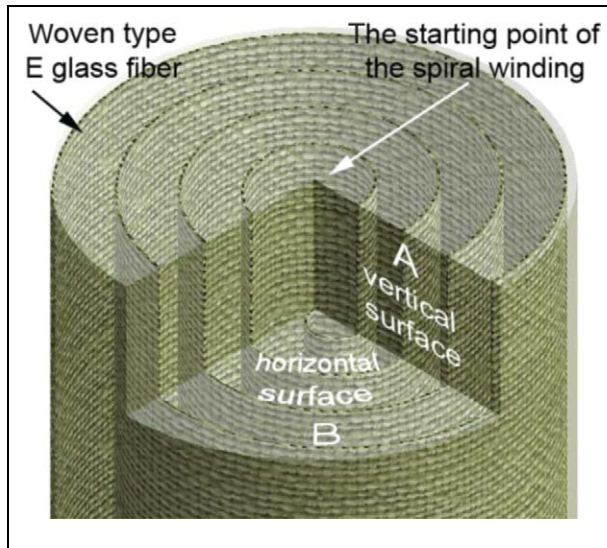


**Figure 7.** Textile-type glass fiber coiling type and “A” and “B” examination surfaces for scanning electron microscope (SEM).

same. Since the allocation of the glass fibers on the surface is always curvilinear, the direction of the fiber is identified as curvilinear.

The SEM image acquired from the second circle is shown in Figure 10, and the zone marked with the  $\phi 2$  sign at a magnification of  $\times 1000$  is shown in Figure 11. The SEM image in Figure 11 is symbolized as  $B\phi 2$ , since it identifies the position related to the horizontal surface. Since all fibers can be viewed as curves, their directions are identified as curvilinear. In the structure, the glass fibers are seen quite clearly. The glass fibers are covered with the matrix material fairly well. In the lower left and upper right parts of the image, the spiral formed of polyester and fiber is visible except for the middle line. The black area points out to the part under the surface level. The black area and the spiral parts are the remaining effects from the surface preparation process. In fact, on the lower part of the surface processed, the compact matrix structure can be viewed free of damage in the arrow directions pointing to the left and the right. The fibers are thoroughly covered with the matrix material.

From the SEM examinations, a composite structure with a fine composition formed in between the glass fiber and the matrix material can be observed. The examination of the structure of glass fiber with a larger zooming ratio can enable a better interpretation. For this purpose, there are two SEM images, the first (Figure 12) is a vertical fiber with magnification of  $\times 3000$  and the second (Figure 13) is the cut view that is vertical to this direction. The purpose is to better determine the space, the fracture or a similar error that could create a disadvantage in terms of resistance of the fiber in the matrix structure. In Figure 12, the glass fiber in the vertical direction can be clearly seen.

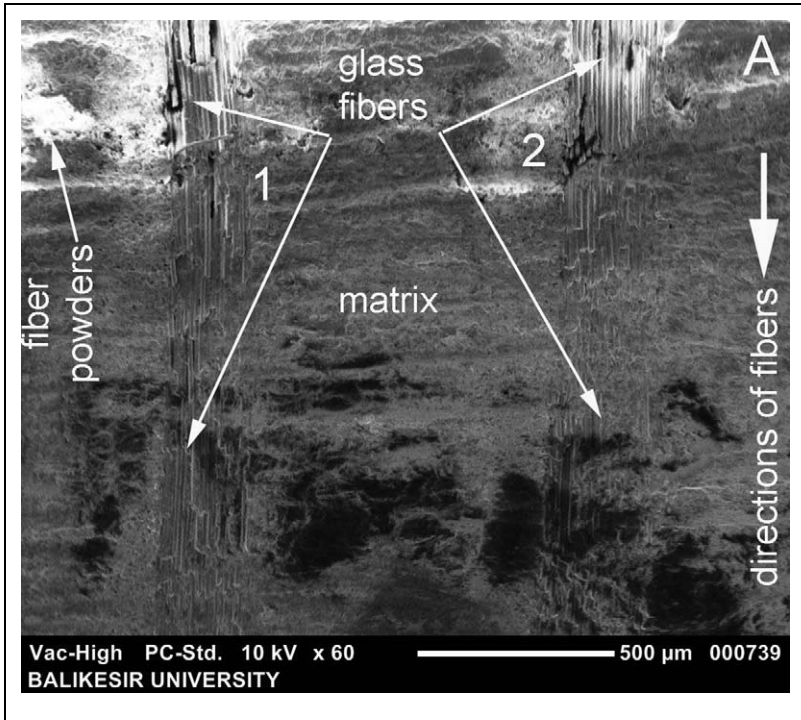


**Figure 8.** Scanning electron microscope (SEM) image of the vertical fibers of the “A” surface.

The structure of the fiber is cylindrical and during the surface preparation process, the polishing process began from the contact point that is tangent to the top surface in the vertical direction to the image plane. It is explicit that the holes are formed on the symmetry axis due to friction occurring during this process. The areas where special attention should be given are the interaction areas of the horizontal fiber with the matrix structure through the external line that determines its diameter. On the image, there are no problematic areas in both corners of the fiber. Figure 13 shows the SEM image acquired from the cut view that is vertical to the fiber. When the diameter of the glass fibers is examined, it is clear that they form a good connection with the matrix structure. No error source that could create problems has been observed. The reason for the bright and white points observed in Figures 12 and 13 is the fiber dust that remains on the surface, despite an appropriate cleaning process.

## Conclusion

Although in a spiral form with a certain degree of leveling, this study examined the effects of woven-type E-glass fiber, which is generally used as a reinforcement material, on compressive stress and density.

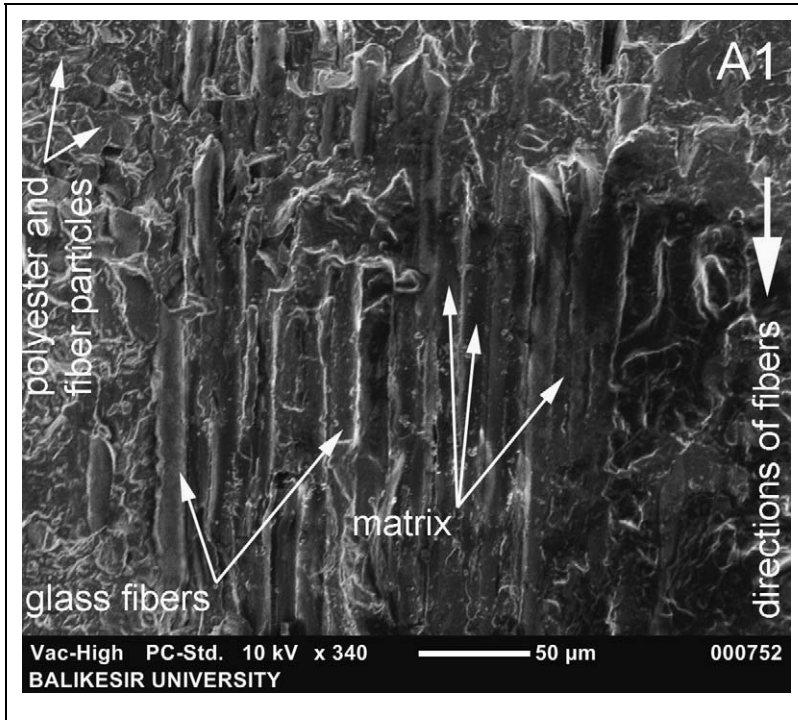


**Figure 9.** Scanning electron microscope (SEM) image of the composite structure of “A1” part.

The application of the smallest interval between spiral wounds of 1 mm results in the highest density structure. Other applications of intervals from 2 mm to 9 mm have also presented very close values. Density largely correlates with the individual densities of each material used in the structure. The length of the spiral E-fiberglass within the composite structure significantly affects the density.

The structure with a 1-mm spiral interval has produced the largest compressive strength. It has been determined that the increasing E-glass fiber length depending on the decreasing spiral interval affects the compression resistance substantially. The lowest compressive strength has been observed on the structure with 6 mm intervals between the spirals. The length of the fiber is greater than 5 mm, and it can be stated that the compressive strength is not related with the fiber length within the structure. In samples with  $\geq 7$  mm spiral intervals, the fiber lengths are very close to each other. Therefore, it can be concluded that the increase in matrix material increases the strength of the composites.

After the compressive tests, pieces of the samples were retain their forms without fragmentation with support of woven fiber structure. Yet a thin outer wall without any reinforcing material deformed as a result of the breakage and cracking of the glassy structure.

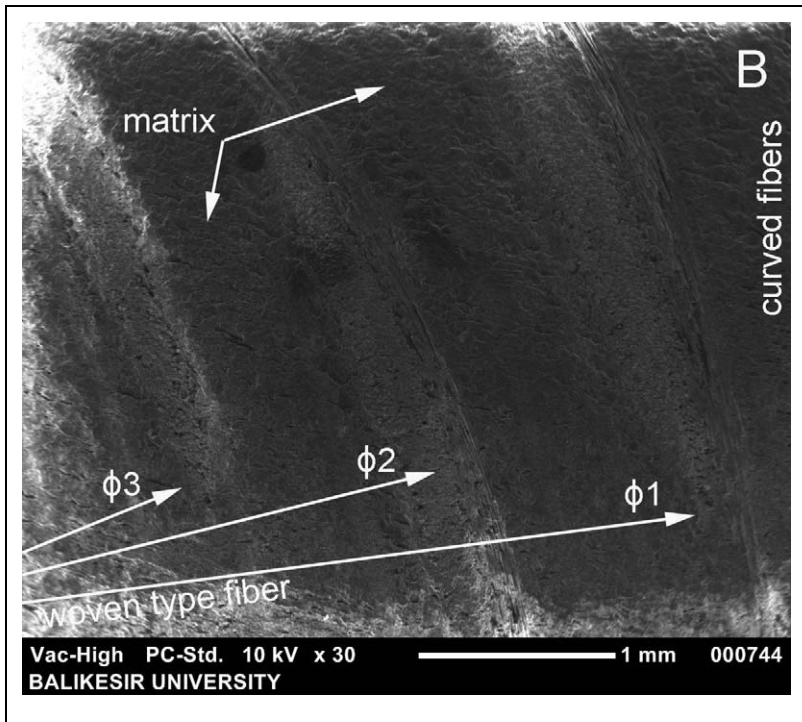


**Figure 10.** Scanning electron microscope (SEM) image of the glass fibers with different diameters on the “B” surface.

It can be asserted that spiral winding can be implemented for composite structures and that the arrangement with the least intervals between the fibers will produce the highest values in terms of compressive strength.

The SEM images parallel and perpendicular to the diameter show that the fibers are covered with matrix material fairly well. Although glass fiber and polyester resin are two different materials, the composite structure is formed with a good composition of them.

Fiber walls are easily covered with the matrix material.

Composite samples are formed of spirally designed fiber arrangements. It has been discovered that glass fiber can be used conveniently as a reinforcement material in a composite material with different designs.

The composite structure can be processed without the need for great strength. During chip removal, each component of the structure can decompose in the form of particles or dust.

Before processing, the matrix material of the structure components is light brown and the fiber is white. After processing, the chip material will have a combination of the two colors. The dominant color here is determined by the dominant color in the component and its amount in the structure.

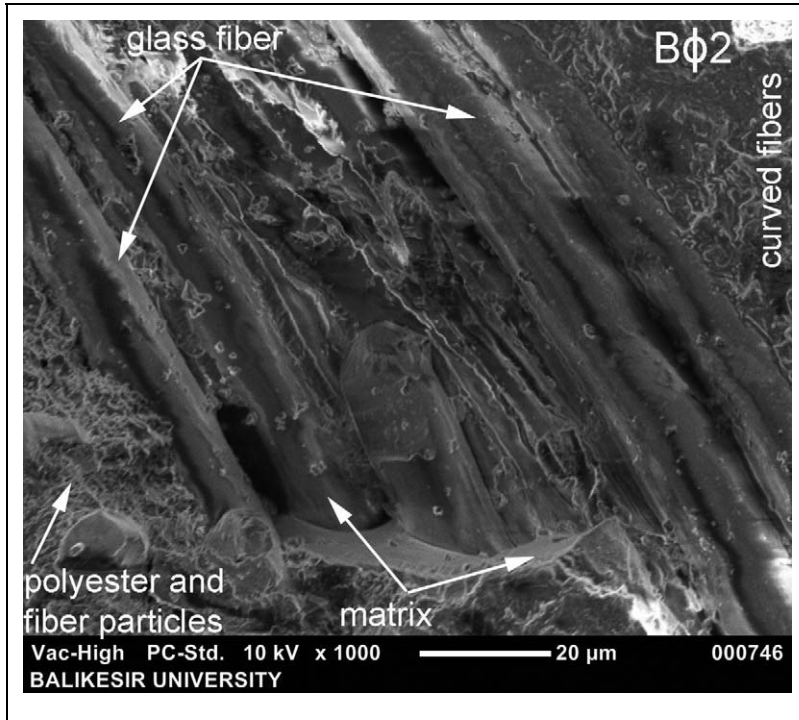


**Figure 11.** Scanning electron microscope (SEM) image of the composite structure of “Bφ2” area.

In this study, the textile-type glass fiber coiled to the axis is deformed with a compression force applied in the direction of the cylinder axis. When the textile-type glass fiber is located on the horizontal plane, by preparing new samples and determining the compression resistance and the changes of intensity, the two cases can be compared. Here, the effect of textile glass fiber on the resistance of the composite in different locations depending on the direction of the load effect can be clearly explained.

### Acknowledgements

The authors are grateful to Balıkesir University, for the use of Research Centre of Applied Sciences (BURCAS), Turkey and to Dr S. K. Akay for his help to use facilities in Microscopy Laboratory, Department of Physic, Faculty of Science and Literature, Uludağ University, Turkey.

### Funding

This work was carried out with the support of The Scientific and Technological Research Council of Turkey (TÜBİTAK) Project No. 108M637.



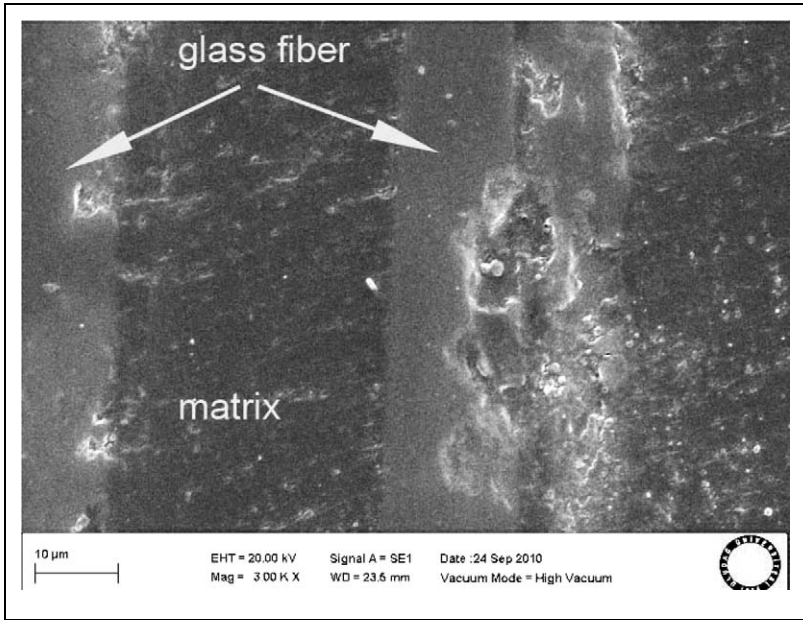


Figure 12. Scanning electron microscope (SEM) image of the fiber in the horizontal position.

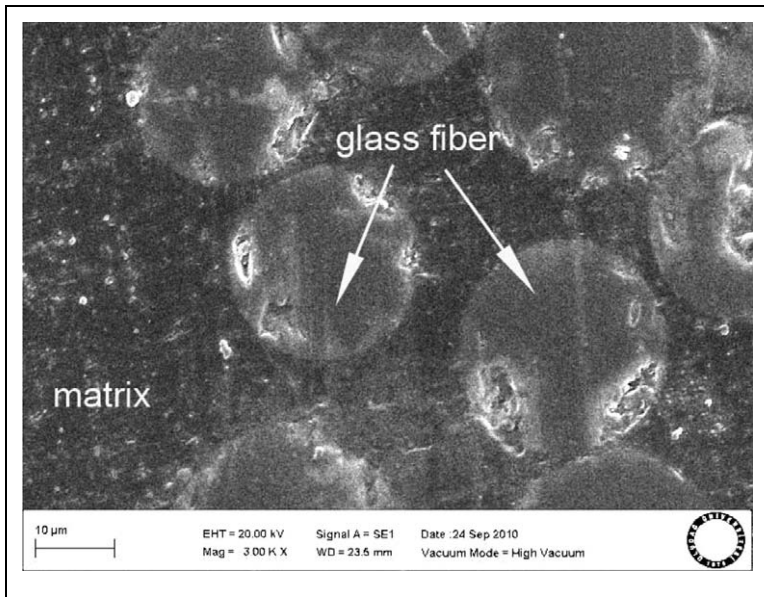


Figure 13. Scanning electron microscope (SEM) image acquired from the cut view that is vertical to the fiber.

## References

1. Kreith F and Goswami D. *The CRC handbook of mechanical engineering*. Washington: CRC Press, 2005.
2. Soh YS, Jo YK and Park HS. Effect of fillers on the mechanical properties of unsaturated polyester resin mortar. In: *Polymers in concrete*. London: E & FN Spon, 1997, pp. 67–74.
3. Rao VVLK and Krishnamoorthy S. Influence of resin and microfiller proportions on strength, density and shrinkage of polyester polymer concrete. *ACI Struct J* 1998; 95: 153–162.
4. Mathukumar M, Mohan D and Rajendran M. Optimization of mix proportions of mineral aggregates using box behnken design of experiments. *Cement Concrete Compos* 2003; 25(7): 751–758.
5. Haffichenari H, Al-Salehi FAR, Al-Hassani STS and Hinton MJ. Effect of temperature on the tensile strength and failure modes of angle ply aramid fibre (KRP) tubes under hoop loading. *Appl Compos Mater* 2002; 9(2): 99–115.
6. Burgueno R, Davol A, Zhao L, Seible F and Karbhari VM. Flexural behavior of hybrid fiber-reinforced polymer/concrete, beam/slab bridge component. *ACI Struct J* 2004; 101(2): 228–236.
7. Varatharajan R, Malhotra SK, Vijayaraghavan L and Krishnamurthy R. Mechanical and machining characteristics of GF/PP and GF/polyester composites. *Mater Sci Eng B* 2006; 132: 134–137.
8. Palanikumar K, Karunamoorthy L and Karthikeyan R. Assessment of factors influencing surface roughness on the machining of glass fiber-reinforced polymer composites. *Mater Design* 2006; 27: 862–871.
9. Zheng Y, Ning R and Zheng Y. Glass fiber-reinforced polymer composites of high compressive strength. *J Reinf Plast Compos* 2004; 23(16): 729–1740.
10. Harris B. The strength of fibre composites. *Composites* 1972; 3(4): 152–167.
11. Abu-Farsaklı GA, Numayr KS and Hamad KhA. A micro-mechanical model the compressive strength of fibrous composite materials. *Compos Sci Technol* 1997; 57(9-10): 1415–1422.
12. Fuping Y, Liren T, Vikas P, Dattatraya D and Rajendran AM. Dynamic shear strength of S2 glass fiber reinforced polymer composites under shock compression. *J Appl Phys* 2008; 103(10): 103537.
13. Deo C and Acharya SK. Solid particle erosion of lantana-camara fiber-reinforced polymer matrix composite. *Polym Plast Technol* 2009; 48: 1084–1087.
14. Ateş E, Aztekin K and Çakır R. Determination of the density and compression strength optimization of without filling material composites. *J Eng Nat Sci* 2010; 28(4): 287–297.
15. DIN 16911, Plastic moulding materials: Polyester resin moulding materials- types- requirements- testing. Germany: The German Institute for Standardization, 1978.
16. DIN 16945, Types of plastic moulding materials: Properties of standard test specimens made of polyester resin compression moulding materials. Germany: The German Institute for Standardization, 1972.
17. DIN 51290-3, testing of polymer concretes (reaction resin concretes) for mechanical engineering purposes: Testing of separately manufactured specimens. Germany: The German Institute for Standardization, 1991.
18. ISO 4012, Concrete-determination of compressive strength of test specimens. Switzerland: International Organization for Standardization, 1978.
19. Aran A. *Fiber-reinforced composite materials*. İstanbul: İTÜ Library, 1990, pp. 420.